Integrated design optimization of wind turbines with noise emission constraints

IOP Conf. Series: Journal of Physics: Conf. Series **1037** (2018) 042005 doi:10.1088/1742-6596/1037/4/042005

Integrated design optimization of wind turbines with noise emission constraints

P Bortolotti[1], CR Sucameli[1], A Croce[2] and CL Bottasso[1,2]

[1] Wind Energy Institute, Technische Universität München, Garching, Germany
[2] Department of Aerospace Science and Technology, Politecnico di Milano, Milano, Italy

E-mail: carlo.bottasso@tum.de

Abstract. This study integrates aeroacoustic noise emission models within a wind turbine design procedure to include overall sound pressure levels as design constraints. The proposed approach aims at the minimization of the cost of energy from wind, while ensuring the compliance with noise emission limits. The reference 3.35 MW onshore wind turbine developed within the international cooperation IEA Wind Task 37 is redesigned to reduce its noise emissions above and below rated wind speed, considering both single- and multi-objective design criteria. Results obtained with the proposed noise-constrained redesign methodology are compared with the simpler approach of reducing the tip speed without altering the blade shape. Results show that, while the simplistic approach causes a drop of -2.8% in annual energy production and a $+2.5\%$ increase in cost of energy, an optimized configuration fulfills the noise requirement without incurring into significant energy penalties.

1. Introduction

The design optimization of a wind turbine is a complex process, and integrated design methodologies are under continuous development to assist designers in their investigations. Among the many goals and constraints that need to be taken into account during design, turbine quietness is assuming an increasing importance due to the combination of both larger rotor sizes and a growing penetration of onshore wind energy. Nonetheless, while the level of detail and complexity of design optimization frameworks is increasing, noise is still typically taken into account only as a limitation on the maximum allowable blade tip speed. This constraint may work as a first approximation, but an approach where noise emission models are fully integrated within the optimization loop is so far lacking. This work aims at filling this gap, including noise emissions within an integrated design approach. The new optimization method should offer the possibility of capturing complex couplings existing between turbine quietness, rotor aerodynamic performance and cost efficiency.

The design approach proposed in this work is developed by expanding the wind turbine design framework `Cp-Max` [1], and it is demonstrated on the redesign of the reference 3.35 MW onshore wind turbine developed within IEA Wind Task 37 [2]. The paper is structured as follows. After this introduction, Sect. 2 presents the frequency-based aeroacoustic models adopted in this study. Next, the algorithmic structures of the design optimization framework are discussed in Sect. 3. The design problems solved with the multi- and single objective optimization approaches are then presented in Sect. 4. Finally, the main conclusions of the work are discussed in Sect. 5.

2. Noise emission models

Aeroacoustic models for the prediction of noise generated by wind turbine blades can be categorized into two families: semi-empirical frequency-domain methods, which are commonly coupled to blade element momentum (BEM) simulation models, and time-domain methods such as the Ffowcs Williams - Hawkings model [3], which are often employed together with 3D CFD models.

`Cp-Max`, as most wind turbine design frameworks, relies on a BEM-based aeroelastic model. Therefore, the present work focuses on frequency-based aeroacoustic models. These are typically subdivided into a family of airfoil self-noise mechanisms and turbulent inflow noise. The first group has been characterized in 1989 by Brooks, Pope and Marcolini [4], who distinguished between turbulent boundary layer - trailing edge (TBL-TE), laminar boundary layer - vortex shedding, trailing edge bluntness, separation-stall and tip noise. The three researchers developed semi-empirical equations for these five self-noise mechanisms, commonly referred to as the BPM model, based on experiments performed with a NACA0012 airfoil at different chord sizes, flow speeds and angles of attack. Among the various sources, TBL-TE and trailing edge bluntness noise are typically considered as relevant noise sources in modern wind turbines. While the former exhibits a wide broadband behavior, the latter emits a tonal noise that can be reduced by limiting the thickness of the trailing edge, especially in the outer span of the blades. A more physical formulation for TBL-TE has later been developed by Parchen [5] at the Dutch research institute TNO, combining Blake's model [6] for the computation of pressure fluctuations with Howe's model [7] for the prediction of far-field sound spectra. This model is commonly named TNO and includes detailed boundary layer characteristics, which can be generated from CFD or by boundary layer solvers. The TNO formulation has finally been recently expanded with work presented in [8].

The second source of noise generated by wind turbines is turbulent inflow (TI) noise, which is generated by pressure oscillations following the unsteady loading generated on the blades caused by the incoming wind turbulence. This was first characterized by Amiet [9] and later further investigated by Lowson [10], Guidati et al. [11] and Moriarty et al. [12]. It should be noted here that the literature on this topic reports several and sometimes slightly conflicting formulations (cf. [13]).

In this work, TBL-TE noise is modelled according to Bertagnolio et al. [8], where the boundary layer characteristics of the airfoils are computed with the software `XFOIL` [14], while the TI noise is modeled adopting the formulation of Amiet [9]. The total noise is assumed to be the sum of the two contributions, so far neglecting other mechanisms of noise generation.

3. Design optimization framework

The frequency-based aeroacoustic models are embedded within the `Cp-Max` framework with the goal of accounting for noise emission limits within a rotor design process. Two integrated rotor design approaches are defined for multi- and single-objective optimization studies. In both approaches, the optimization variables are represented by the four aerostructural parameters Σ_c, T_c, $\Sigma_{t/c}$ and $T_{t/c}$, which control the blade planar and transversal shapes [1] and that are defined as:

$$\Sigma_c = \frac{3A_b}{A} = \frac{3\int_0^R c(r)\,\mathrm{d}r}{\pi R^2}, \tag{1a}$$

$$T_c = \frac{\int_0^R rc(r)\,\mathrm{d}r}{A_b}, \tag{1b}$$

$$\Sigma_{t/c} = \frac{1}{100}\int_0^1 t/c(\eta)\,\mathrm{d}\eta, \tag{2a}$$

$$T_{t/c} = \frac{\int_0^1 \eta t/c(\eta)\,\mathrm{d}\eta}{\int_0^1 t/c(\eta)\,\mathrm{d}\eta}, \tag{2b}$$

where A_b is the blade planform area, A is the rotor swept area, c the chord, r is the dimensional blade span, t/c is the blade relative thickness and η the non-dimensional blade span.

3.1. Multi-objective optimization

In the multi-objective design approach, which is schematically shown in Fig. 1, an aerodynamic optimization is run for each instantiation of the four optimization variables Σ_c, T_c, $\Sigma_{t/c}$ and $T_{t/c}$. In the blade aerodynamic design step, the blade outer shape is parameterized in terms of chord

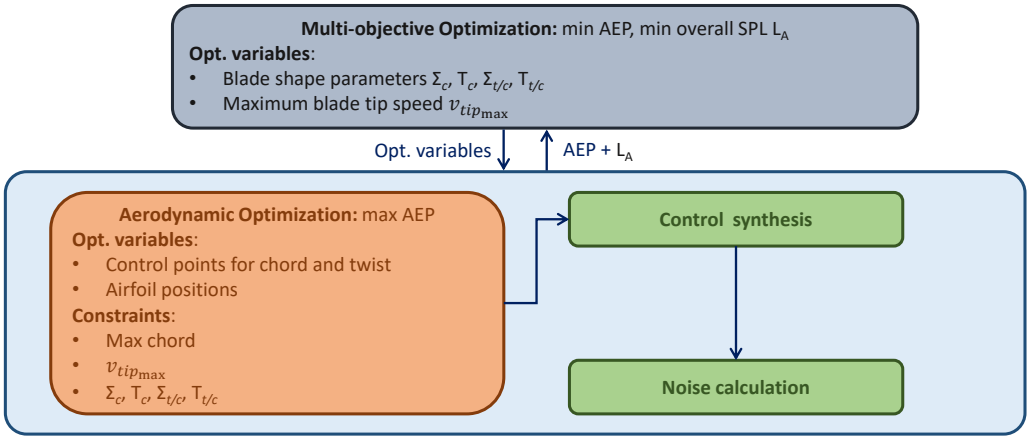

Figure 1: Algorithmic architecture of the multi-objective design optimization process.

and twist distributions, as well as airfoil spanwise positions. These quantities are optimized for maximum annual energy production (AEP), while respecting inequality constraints on maximum chord and maximum blade tip speed $v_{tip_{\max}}$, as well as equality constraints fixing the values of Σ_c, T_c, $\Sigma_{t/c}$ and $T_{t/c}$. The optimum aerodynamic shape is then used to tune a model based controller and to quantify the noise emission. This is expressed in terms of overall A-Weighted sound pressure level L_A. L_A is obtained from the summation of the relative 1/3 octave band spectra weighted through an A-Type frequency filter, which takes into account the non-linear human hearing response to noise. The spectra are computed from a simplified aeroelastic simulation assuming a steady wind speed of 9 m/s. AEP and L_A are the two merit figures of a non-dominated sorting genetic algorithm `NSGA-II` [18] implemented in `Matlab` [19]. The output of the optimization is a Pareto front identifying all trade-offs that maximize AEP and minimize L_A. Notably, in order to reduce the computational costs, no structural optimization is performed and the properties describing the elastic characteristics of the blades are kept constant. The underlying assumption here is the limited effect of the blade structure on both AEP and L_A.

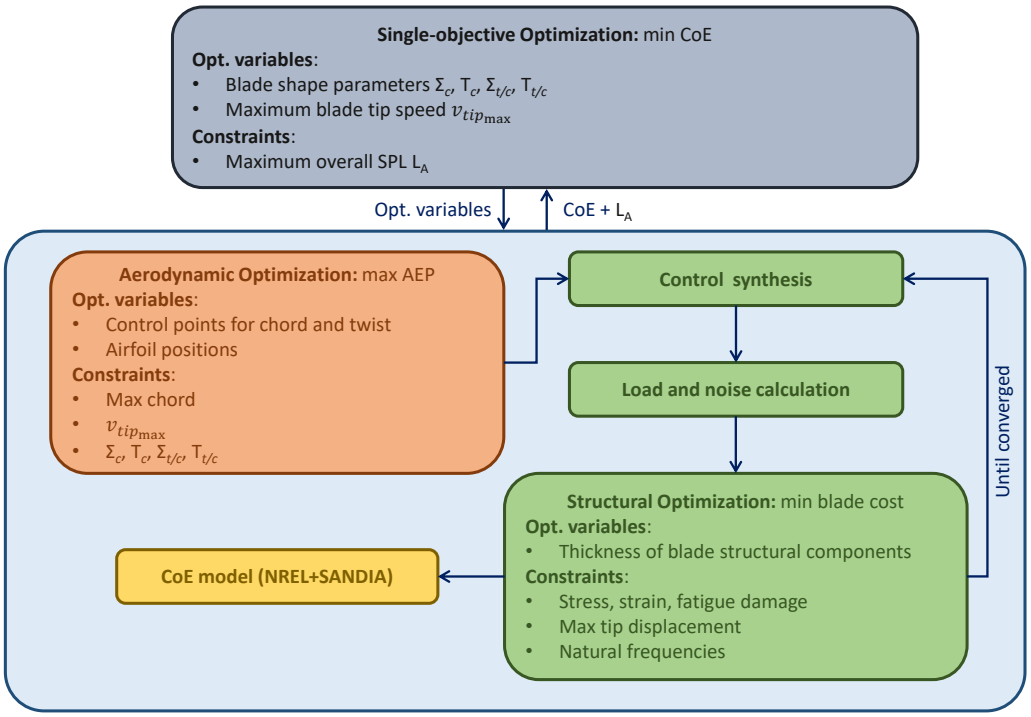

Figure 2: Algorithmic architecture of the single-objective design optimization process.

3.2. Single-objective optimization

In the single-objective design approach, which is schematically shown in Fig. 2, the set of four optimization variables is augmented with the maximum allowable blade tip speed $v_{tip_{\max}}$. Here, the turbine design problem minimizes the single merit figure of cost of energy (CoE), which is computed from the combination of two cost models developed at NREL [15] and at SANDIA National Laboratories [16]. The latter estimates blade cost, whose value is used by the former model to estimate the CoE. The CoE is obtained by stacking in sequence the same aerodynamic optimization presented in Sect. 3.1 and reported in Fig. 1 and a detailed blade structural design loop. This aims at minimizing blade cost by sizing the spanwise thickness of the various structural components, including spar caps, outer shell skin, shear web skin and leading and trailing edge reinforcements. The structural design complies with limits on ultimate stresses and strains, fatigue damage, frequency constraints and minimum tower clearance. In addition, the thickness of the core of the sandwich panels in the outer shell and in the shear webs is sized to prevent buckling of the panels. The ultimate and fatigue loads driving the structural blade sizing are computed by iteratively running a relevant subset of design load cases [1]. In the single-objective optimization approach, the gradient-based optimization solver implemented in function `fmincon` of `Matlab` [19] is used to identify the minimum CoE.

4. Design studies

Two families of design studies are conducted based on the IEA Task 37 3.35 MW onshore wind turbine, briefly described in Sect. 4.1. At first, a Pareto front is generated for the multi-objective optimization of maximum AEP and minimum L_A. Secondly, a single-objective optimization is conducted for minimum CoE. The two design studies are presented in Sect. 4.2 and Sect. 4.3,

Table 1: Configuration of the baseline 3.35 MW wind turbine.

Data	Value	Data	Value
Wind class	IEC 3A	Rated electrical power	3.35 MW
Rated aerodynamic power	3.60 MW	DT & Gen. efficiency	93.0%
Hub height H	110.0 m	Rotor radius R	65.0 m
Cut-in wind speed V_{in}	4 m/s	Cut-out wind speed V_{out}	25 m/s
Rotor cone angle Ξ	3.0 deg	Nacelle uptilt angle Φ	5.0 deg
Rotor planar solidity Σ_c	4.09%	Max blade tip speed $v_{\mathrm{tip}_{\max}}$	80.0 m/s
Blade mass	17,404 kg	Tower mass	553 ton
Blade cost	123.9 k$	Tower cost	829.8 k$
Nominal AEP	13.95 GWh	Turbulent AEP (DLC 1.1)	13.03 GWh
ICC	4,155.0 k$	CoE (Turbulent AEP)	46.87 $/MWh

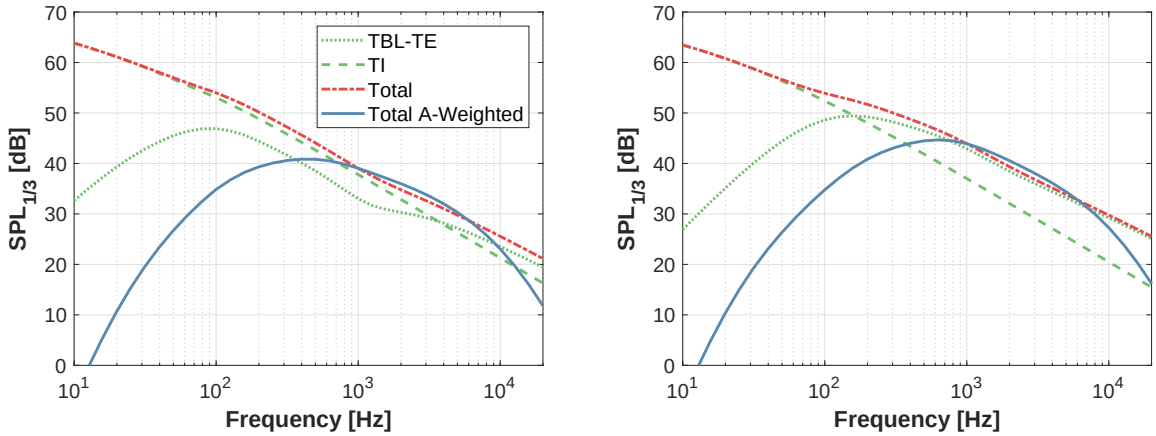

(a) Wind speed = 7 m/s (b) Wind speed = 13 m/s

Figure 3: Noise spectra computed between 10 Hz and 20 kHz at wind speeds of 7 m/s and 13 m/s for the baseline configuration of the 3.35 MW wind turbine.

respectively.

4.1. The 3.35 MW onshore wind turbine

The design studies are developed adopting as starting point a reference 3.35 MW onshore wind turbine equipped with a rotor diameter of 130 meters and a hub height of 110 meters. The principal configurational parameters of the wind turbine are reported in Table 1. The baseline machine has a maximum allowable blade tip speed $v_{tip_{\max}}$ of 80 m/s. Figure 3 shows the noise emissions computed in 30 seconds of standard DLC 1.1 at hub height with wind speeds equal to 7 m/s and 13 m/s. The observer position is set as prescribed by the IEC61400-11 standards [17], namely downwind on the ground at a distance from tower base equal to the turbine total height. Results are expressed as sound pressure levels (SPL) expressed in dB. Notably, TI dominates the spectrum at 7 m/s, while TBL-TE is the prevailing mechanism at 13 m/s. The L_A values equal 51.0 dB(A) and 54.5 dB(A) for the two wind speeds respectively.

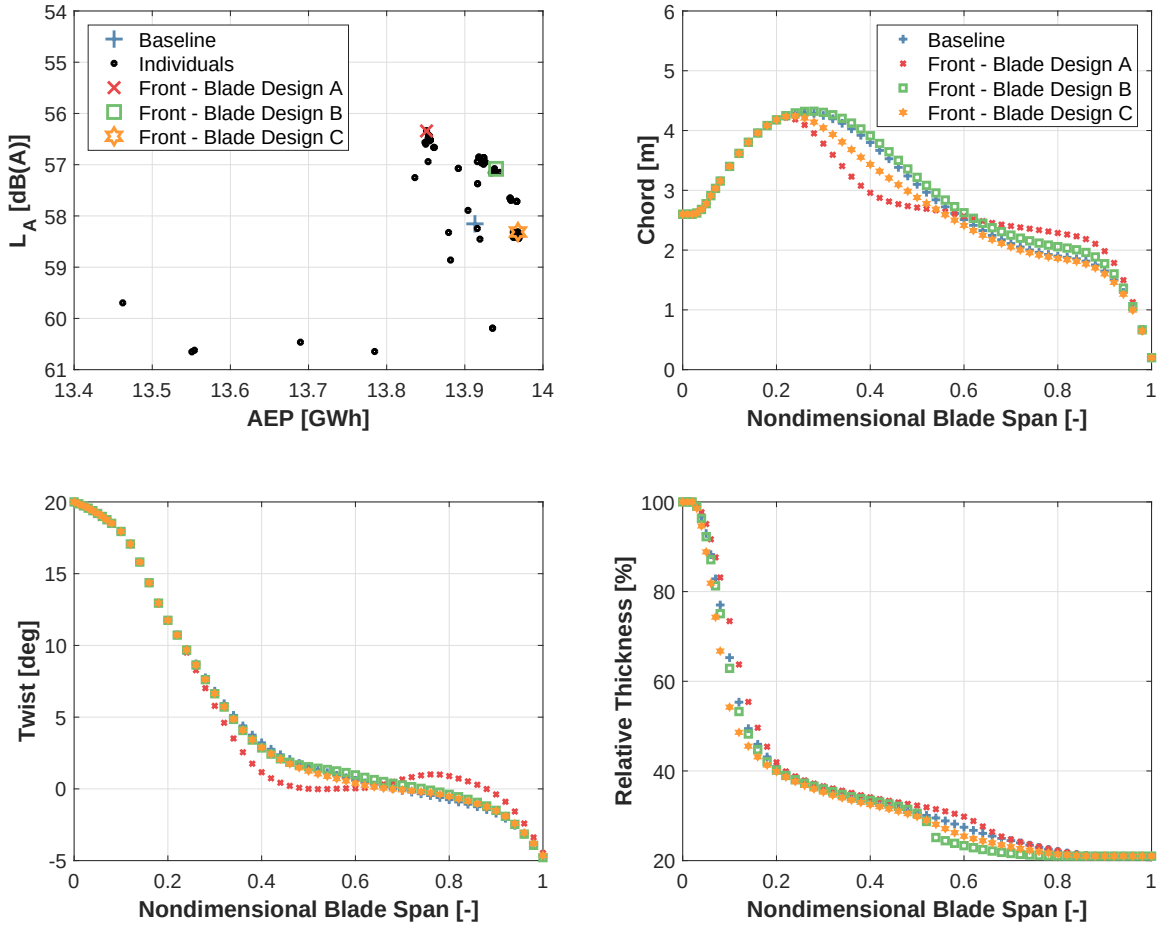

Figure 4: Results of the multi-objective genetic optimization for maximum AEP and minimum L_A.

4.2. Multi-objective optimization

A first study aiming at the characterization of the solution space is conducted by running the multi-objective design process discussed in Sect. 3.1. Results are reported in Fig. 4. The optimization converges to a Pareto front after 6 generations of 20 individuals each. The various solutions are characterized by different blade shapes, where exemplary solutions named Blade Design A, B and C are highlighted. The three blade aerodynamic shapes differ in terms of chord, twist and relative thickness distributions. The most marked effect is visible in the chord distribution, which in `Cp-Max` has a direct impact on the tip speed ratio (TSR) and therefore on the rotational speeds adopted below rated wind speed. The solutions generating high AEP are characterized by low values of both Σ_c and T_c, while a lower noise emission is associated to higher values of chord in the outer portion of the blade. This effect is clearly visible in Blade Design A. Below rated conditions, the blade operates at a TSR lower than the one of the baseline design. Thanks to the lower rotational speeds, L_A is reduced, at the cost of a lower AEP. An opposite effect is instead observed in Blade Design C, where a lower solidity is aerodynamically advantageous, resulting however in a higher TSR and consequently higher L_A.

In the results, the effect of the two parameters $\Sigma_{t/c}$ and $T_{t/c}$ influencing the blade relative thickness is less clear. This is likely due to the more limited freedom of the aerodynamic

optimizer in changing the relative thickness. Indeed, the aerodynamic optimizer in `Cp-Max` can so far only move a given profile along the span, while it cannot change the shape of a profile. Finally, the twist distributions reported in the bottom left corner of Fig. 4 are simply the ones optimizing the AEP for each combination of chord and airfoil positioning.

4.3. Single-objective optimization

Next, two studies are conducted adopting the single-objective optimization process presented in Sect. 3.2. The structural loop, which —differently from the previous case— is now present, uses loads computed from 52 different DLCs representing normal operating conditions, extreme turbulent wind conditions, the occurrence of extreme gusts combined with electric faults and, finally, the occurrence of a 50-year storm at different values of yaw angle. These are a subset of the drivers for this machine, as identified during the IEA Wind Task 37 design process.

In the first of the two design problems, L_A is measured during 30 seconds of turbulent wind at an average speed of 7 m/s (i.e. in the partial load region), and it is constrained to be reduced by 1 dB(A), lowering the turbine noise emissions to 50 dB(A). A simplistic approach to this problem consists in lowering the TSR for the baseline rotor configuration. However, this has the effect of reducing the TSR from the optimal value of 8.2 to an aerodynamically sub-optimal value of 7.5. This causes significant losses in AEP, which is in turn lowered by 2.8% when measured in turbulent wind conditions in DLC 1.1. This reduction in AEP results in a considerable increase in CoE of 2.5%.

A better alternative to the simplistic approach consists in optimizing the blade shape parameters Σ_c, T_c, $\Sigma_{t/c}$ and $T_{t/c}$ together with $v_{tip_{\max}}$, subject to an inequality constraint limiting L_A to be smaller than 50 dB(A). After four iterations, the optimizer converges to the solution reported in Fig. 5. Thanks to the larger chord in the outer portion of the blades, the rotor spins at a TSR equal to 7.6, leading to a slight increase in AEP of less than 0.1%. In addition, $v_{tip_{\max}}$ is reduced to 75 m/s. This helps limiting loads and blade cost, with only a minor impact on AEP. Overall, the newly designed blade is 1.0% more expensive than the baseline configuration, while CoE is increased, but only by a negligible +0.05%. As already observed in past studies [1], the solution space of CoE at frozen rotor diameter is indeed very flat and multiple neighboring solutions are often characterized by very similar CoE values. However, in this case the addition of the noise constraint is a clear design driver, which leads to a solution that is strongly characterized by its presence.

Finally, a second single-objective optimization design study is conducted, where L_A generated with a turbulent average wind speed of 13 m/s, i.e. in the full power region, has to be reduced from 54 dB(A) to 51 dB(A). Here, the optimization satisfies the limit on L_A by reducing $v_{tip_{\max}}$ to 68 m/s. The lower $v_{tip_{\max}}$ generates losses in AEP equal to 1.2%, but leads to savings in blade cost of 7.1% thanks to the reduced loads. Overall, CoE is estimated to increase by 0.3%. Two notable aspects of this last study should be discussed. First, differently from the partial load case, the solution is here obtained without consistent variations in the blade shape. The optimizer is indeed again victim of the flatness of the CoE solution space, and the four parameters undergo small variations with no marked effect neither on the noise constraint nor on the CoE. Secondly, the NREL cost model may here neglect an increase of the drive train costs, which are likely to occur given the 15% change in the rated values of rotational speed and shaft torque.

5. Conclusions

This work proposes a novel integrated design procedure to minimize cost while complying with noise emission limits. Results from the re-optimization of a reference 3.35 MW onshore wind turbine show that the solutions computed by the proposed optimization approach differ from the ones found without aeroacoustic noise limits. The blade planar shape is particularly affected when the noise reduction is enforced in the partial load region, while only modest effects are

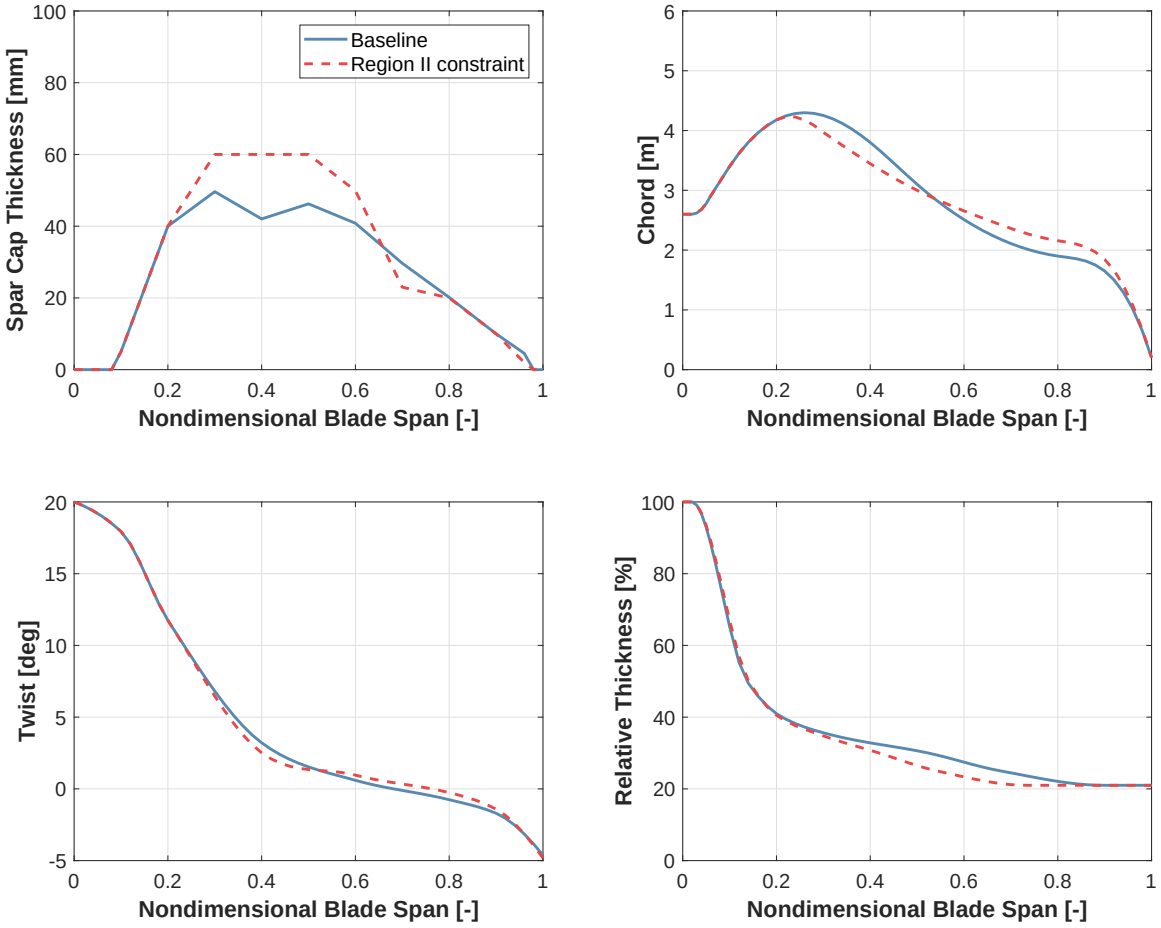

Figure 5: Results of the single-objective gradient-based optimization for minimum CoE.

observed for the full load regime. The study also considers the simpler approach of reducing noise by limiting tip speed, which is a classical solution implemented for example at night for turbines installed in proximity of populated areas. This approach, although simple and effective, results in inevitable energy losses.

Work is currently progressing to validate the TI and TBL-TE noise emission models with experimental measurements. In addition, new optimization algorithms are being tested to introduce additional degrees of freedom as well as couplings. Focus is especially dedicated to the twist and TSR, which in the current framework are set to be the aerodynamic optima, while noise and load mitigation may favor sub-optimal configurations.

Acknowledgements

This research was partially supported by the German Federal Ministry for Economic Affairs and Energy (BMWi) within the TremAc (FKZ: 0325839D) project.

References

[1] Bortolotti P, Bottasso CL, Croce A. Combined preliminary-detailed design of wind turbines. *Wind Energy Science*, 2016;1(1):71-88. doi: 10.5194/wes-1-71-2016

[2] Dykes K, Rethore PE, Zahle F, Merz K. Wind Energy Systems Engineering: Integrated RD&D. IEA Task 37 Final Proposal, 2015. https://sites.google.com/site/ieawindtask37/

[3] Ffowcs Williams JE, Hawkings DL. Sound generation by turbulence and surfaces in arbitrary motion. *Philosophical Transactions of the Royal Society of London*, 1968;264(1151). doi: 10.1098/rsta.1969.0031
[4] Brooks TF, Pope DS, Marcolini MA. Airfoil self-noise and prediction. *NASA Reference Publication 1218*, 1989.
[5] Parchen RR. Progress report draw : a prediction scheme for trailing edge noise based on detailed boundary layer characteristics. *Report TNO Institute of Applied Physics*, Delft, The Netherlands, 1998.
[6] Blake W. Mechanics of Flow-Induced Sound and Vibration, Volume 1: General Concepts and Elementary Sources. 2nd Edition, Academic press, 2017. ISBN 9780128122891
[7] Howe MS. A review of the theory of trailing edge noise. *Journal of Sound and Vibration*, 1978;61(3):437-465. doi: 10.1016/0022-460X(78)90391-7
[8] Bertagnolio F, Madsen HA, Fischer A. A combined aeroelastic-aeroacoustic model for wind turbine noise: verification and analysis of field measurements. *Wind Energy*, 2017;20(8):1331-1348. doi: 10.1002/we.2096
[9] Amiet RK. Acoustic radiation from an airfoil in a turbulent stream. *Journal of Sound and Vibration*, 1975;41(4):407-420. doi: 10.1016/S0022-460X(75)80105-2
[10] Lowson MV. Assessment and prediction of wind turbine noise. *Flow Solutions Report 92/19*, 1993.
[11] Guidati G, Bareiss R, Wagner S, Dassen T, Parchen R. Simulation and measurement of inflow-turbulence noise on airfoils. *3rd AIAA/CEAS Aeroacoustics Conference*, Atlanta,GA, 1997. doi: 10.2514/6.1997-1698
[12] Moriarty P, Guidati G, Migliore P. Prediction of turbulent inflow and trailing-edge noise for wind turbines. *11th AIAA/CEAS Aeroacoustics Conference*, Monterey, CA, 2005. doi: 10.2514/6.2005-2881
[13] Sucameli CR, Bortolotti P, Croce A, Bottasso CL. Comparison of some wind turbine noise emission models coupled to BEM aerodynamics. *The Science of Making Torque from Wind 2018*, Milano, Italy, 2018.
[14] XFOIL Documentation, 2017 http://web.mit.edu/drela/Public/web/xfoil/
[15] Fingersh L, Hand M, Laxson A. Wind turbine design cost and scaling model. *NREL Technical Report* NREL/TP-500-40566, 2006.
[16] Johans W, Griffith DT. Large Blade Manufacturing Cost Studies Using the Sandia Blade Manufacturing Cost Tool and Sandia 100-meter Blades, Sandia National Laboratories, *SANDIA Technical Report*, 2013.
[17] Wind turbine generator systems - part 11: Acoustic noise measurement techniques. International Standard IEC 61400-11, 2006.
[18] Deb K, Pratap A, Agarwal S, Meyarivan T. A Fast and Elitist Multiobjective Genetic Algorithm: NSGAII. *IEEE Transactions on Evolutionary Computation*, 2002.
[19] `Matlab`. The MathWorks Inc., 3 Apple Hill Drive, Natick, MA 01760-2098, USA, `www.mathworks.com`